

**High organic carbon burial but high potential for methane ebullition in the
sediments of an Amazonian hydroelectric reservoir**

Gabrielle R. Quadra¹✉, Sebastian Sobek², José R. Paranaíba¹, Anastasija Isidorova²,
Fábio Roland¹, Roseilson do Vale³, Raquel Mendonça¹

¹ Laboratório de Ecologia Aquática, Programa de Pós-Graduação em Ecologia,
Universidade Federal de Juiz de Fora, 36036 900, Brazil.

² Department of Ecology and Genetics, Limnology, Uppsala University, 752 36,
Sweden.

³ Universidade Federal do Oeste do Pará, Instituto de Engenharia e Geociências, 68040
255, Brazil.

✉gabrielle.quadra@ecologia.ufjf.br

Abstract

Reservoir sediments sequester significant amounts of organic carbon (OC), but at the same time, high amounts of methane (CH₄) can be produced and emitted during the degradation of sediment OC. While the greenhouse gases emission of reservoirs has received a lot of attention, there is a lack of studies focusing on OC burial. In particular, there are no studies on reservoir OC burial in the Amazon, even though hydropower is expanding in the basin. Here we present results from the first investigation of OC burial and CH₄ concentrations in the sediments of an Amazonian hydroelectric reservoir. We performed sub-bottom profiling, sediment coring and sediment pore water analysis in the Curuá-Una reservoir (CUN; Amazon, Brazil) during rising and falling water periods. Spatially resolved average sediment accumulation rate was 0.6 cm yr⁻¹ and a average OC burial rate was 91 g C m⁻² yr⁻¹. This is the highest OC burial rate on record for low-latitude hydroelectric reservoirs. Such high rate probably results from a high OC deposition onto the sediment, which compensates the high OC mineralization at 28-30°C water temperature. Elevated OC burial was found near the dam, and close to major river inflow areas. C:N ratios between 10.3 and 17 (average ± SD: 12.9 ± 2.1) suggest that both land-derived and aquatic OC accumulate in CUN sediments. About 23% of the sediment pore water samples had dissolved CH₄ above the saturation concentration. This represents a higher share than in other hydroelectric reservoirs, indicating a high potential for CH₄ ebullition, particularly in river inflow areas.

Keywords: Amazon, carbon cycling, C:N ratio, dam, pore water, river inflow

Introduction

Although freshwater ecosystems represent a small fraction of the global area (~4% of terrestrial area) (Downing et al., 2012; Verpoorter et al., 2014), they play an important role in the global carbon cycle, both emitting carbon to the atmosphere and burying carbon in the sediments (Cole et al., 2007; Tranvik et al., 2009). Many studies have been conducted on inland water carbon emissions, while the organic carbon (OC) burial in inland water sediments is comparatively understudied on a global scale (Raymond et al., 2013; Mendonça et al., 2017). Since a part of the buried OC may offset a share of greenhouse gas emission, it is essential to include OC burial in the carbon balance of inland water ecosystems (Kortelainen et al., 2013; Mendonça et al., 2017).

Freshwater OC burial rate varies both in space and time due to many factors, such as land cover, hydrological conditions, OC and nutrient input and climate change (Radbourn et al., 2017; Stratton et al., 2019). Several studies have shown that reservoirs bury more OC per unit area than lakes, rivers and oceans (Mulholland and Elwood, 1982; Mendonça et al., 2017), which may be attributed to the high sedimentation rate caused by the extensive sediment trapping when water flow is dammed (Vörösmarty et al., 2003). Considering the importance of reservoirs as a carbon sink (~28 to 55% of total inland water OC burial; Mendonça et al., 2017) and the increasing number of hydroelectric dams (Zarfl et al., 2015), the limited number of studies on OC burial in reservoirs severely hampers the understanding of this important component in the carbon balance of the continents (Mendonça et al., 2017). In particular, large regions of the Earth are at present completely unsampled concerning inland water carbon burial. Approximately 90% of the sites sampled for carbon burial are in North America and Europe, while there are only few measurements in South American, African and Asian countries (Mendonça et al., 2017).

To the best of our knowledge, OC burial has so far not been studied in an Amazonian reservoir. However, it is likely that reservoirs in tropical rain forest areas bury OC at a comparatively high rate, as temperature and runoff were identified as important drivers of OC burial in lakes and reservoirs (Mendonça et al., 2017). Indeed, OC burial in Amazonian floodplain lakes was reported to be much higher than in other lakes (Sanders et al., 2017). Moreover, many new hydropower dams are planned in the Amazon due to the high potential of the area for hydroelectricity (da Silva Soito and Freitas, 2011; Winemiller et al., 2016). However, there is currently no data to gauge the potential effect of hydropower expansion in the Amazon on carbon burial.

Besides the significant potential of trapping OC in the sediment, reservoirs can be strong sources of methane (CH_4) to the atmosphere (Deemer et al., 2016). Several studies have shown a positive relationship between CH_4 production and temperature in freshwater ecosystems (Marotta et al., 2014; Wik et al., 2014; Yvon-Durocher et al., 2014; DelSontro et al., 2016; Aben et al., 2017), and also organic matter supply to sediment is an important regulator of CH_4 production and emission (Segers, 1998; Sobek et al., 2012; Grasset et al., 2018). Thus, tropical reservoirs, especially those situated in highly productive humid tropical biomes, such as the Amazon, may produce more CH_4 than temperate ones due to higher annual temperatures and availability of organic matter in their sediments (Barros et al., 2011; Mendonça et al., 2012; Fearnside and Pueyo, 2012; Almeida et al., 2013), although highly-emitting reservoirs can also be situated in temperate regions (Deemer et al., 2016). Further, in many reservoirs, CH_4 ebullition (i.e., emission of gas bubbles) is an important or dominant emission pathway, but it is very difficult to measure due to its strong variability in space and time (McGinnis et al., 2006; Deemer et al., 2016). Measurements of dissolved CH_4 concentration in sediment pore water may, therefore, help to identify if ebullition is

likely to occur (CH_4 concentrations close to the sediment pore water saturation), and thus to judge if the sediments act mainly as carbon sinks, or also as CH_4 sources. While CH_4 emission typically constitutes a very small flux in terms of carbon mass, it is highly relevant to climate since CH_4 is a ~34 times stronger greenhouse gas than CO_2 (IPCC, 2013). The transformation of sediment OC (i.e. previously fixed CO_2) to atmospheric CH_4 therefore represents an amplification of radiative forcing in the atmosphere.

Both OC burial and CH_4 production take place in sediments. Here, we present results of a study approaching these processes on sediments of an Amazonian hydroelectric reservoir during hydrologically different seasons, which was motivated by an absence of such studies even though sediment carbon processing in Amazonian reservoirs may potentially be high. We aimed at providing a spatially-resolved quantification of OC burial, as well as a mapping of CH_4 saturation in the sediment porewater, which is indicative of the potential occurrence of CH_4 ebullition. Thereby, this study is intended to contribute to improved understanding of the potential biogeochemical effects of the current expansion of hydropower (Almeida et al., 2019) on the Amazonian carbon budget.

Material and methods

Study area

Curuá-Una is an Amazonian reservoir (CUN; 2°50' S 54°18' W) located in the Pará state (North of Brazil), created in 1977, and used mainly to produce energy. The average water depth of CUN is 6 m (Fearnside, 2005; Paranaíba et al., 2018) and it has a maximum flooded area of 72 km² (Duchemin et al., 2000; Fearnside, 2005). The main tributary is the Curuá-Una River, contributing with most of the reservoir's water discharge (57.4%), but rivers Moju (11.7%), Mojuí (4.4%), Poraquê (3.2%) and other

small ones (2.9%) are also important (Fearnside, 2005). While tropical rain forest covers 90.8% of the total CUN catchment area, managed lands, which covers 8.9% of the total catchment, contribute with a high share (up to 41%) of the land cover in some sub-catchments (**Fig. 1**).

The reservoir is characterized by a high amount of flooded dead trees (area with trees covers ~90% of the total reservoir area), which may be expected to decrease water flow and promote sedimentation. According to a previous study (Paranaíba et al., 2018), CUN is oligotrophic (total nitrogen (TN): 0.7 mg L^{-1} , average; total phosphorus (TP): 0.02 mg L^{-1} , average), the surface water is warm (average \pm SD: $30.1 \pm 1.4 \text{ }^{\circ}\text{C}$), slightly acidic (pH of 6.1 ± 0.7), with low conductivity ($16 \pm 11 \text{ }\mu\text{S cm}^{-1}$) and moderately oxygenated ($6.7 \pm 1.9 \text{ mg L}^{-1}$).

Sampling

We carried out two samplings in the CUN reservoir. In February 2016, during the rising water period (**Fig. S1**), we used an Innomar SES-2000 parametric sub-bottom profiler operating at 100 kHz (primary frequency) and 15 kHz (secondary frequency) to determine the bathymetry and sediment thickness from which we planned to acquire spatially resolved sediment accumulation rates and OC burial rate, similar to Mendonça et al. (2014). Sediment thickness was difficult to observe with the sub-bottom profiler, though, presumably because of the widespread presence of gas bubbles in the sediment which reflect the sound waves very efficiently, preventing them from reaching the sub-bottom layer. Therefore, OC burial rates were determined from sediment cores only. In September 2017, during the falling water period (**Fig. S1**), additional sediment cores were then taken to cover the reservoir as much as possible.

We took a total of 114 sediment cores during the two sampling occasions, approximately evenly distributed along the reservoir, both longitudinally and laterally, to measure sediment thickness and, thus, estimate sediment accumulation and OC burial rates (**Fig. 1, Table S1**). Cores were retrieved using a gravity corer equipped with a hammer device (UWITEC, Mondsee, Austria) to sample the entire sediment layer, including the pre-flooding material. The layer of transition between post- and pre-flooding material was visually identified. Visual identification is possible because the moment when the reservoir was flooded is the onset of a lacustrine depositional regime, which is characterized by different sediment texture and composition in relation to the pre-flooding soil or fluvial sediment (**Fig. S2**). The thickness of the post-flooding sediment was noted in all cores and used to calculate sediment accumulation rates ('data analysis'). Nineteen sediment cores, from sites spread out evenly over the reservoir were sliced in 2 cm thick slices and dried at 40 °C for further laboratory analysis. The samples were weighed before and after drying and the results are, then, expressed in dry weight.

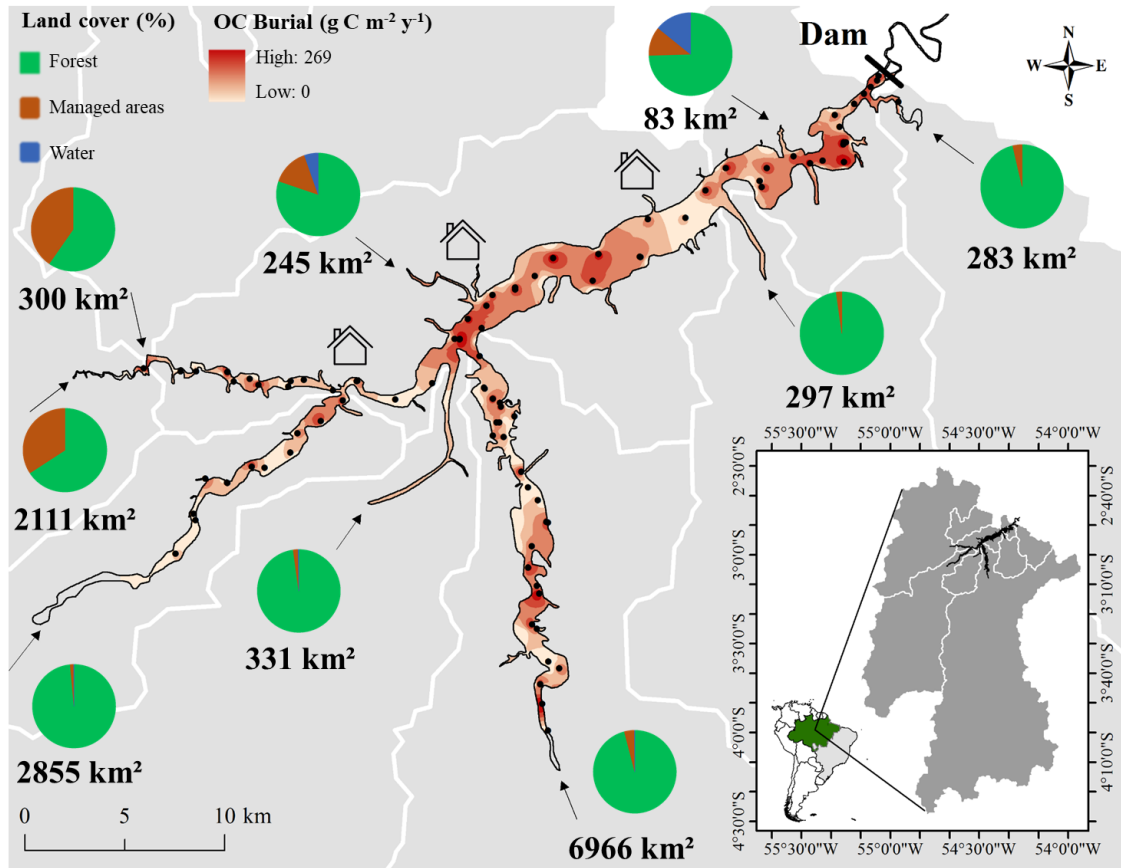


Figure 1. Organic carbon burial rate (OC burial; $\text{g C m}^{-2} \text{ yr}^{-1}$) of the Curuá-Una reservoir. The circles show the land cover of each sub-catchment, delineated by white lines. The numbers near the circles show the area in km^2 for each sub-catchment. The black dots represent the sediment sampling sites to estimate OC burial rates. The arrows represent the main river inflows. The houses represent settlements at the reservoir. The bottom-right map shows the location of the reservoir in Brazil (the green area is the Brazilian Amazon region) and the total extension of each sub-catchment.

In both sampling campaigns, targeted to rising and falling water periods, sediment cores were taken for the analysis of pore water CH_4 concentration profiles ($n = 16$ in February 2016 and $n = 9$ in September 2017). Of the nine cores taken in September 2017, eight were situated at sites previously sampled in February 2016, to compare the CH_4 concentrations between sampling occasions. It is difficult to sample

the exact same location at different periods due to the water level changes, GPS error and boat drifting. Thus, the repeated samplings at these eight sites were within < 100 m distance.

Water temperature and dissolved oxygen profiles were measured with a multiparameter sonde (YSI 6600 V2) in a total of 28 depth profiles, distributed across the reservoir at both sampling occasions. Air pressure and temperature were measured with a portable anemometer (Skymaster SpeedTech SM-28, accuracy: 3%), water depth was measured with a depth gauge (Hondex PS-7), and sediment temperature with a thermometer (Incoterm), which was inserted into the sediment right after core retrieval.

Carbon and nitrogen analysis

OC and TN concentrations were determined in a sub-set of 19 cores, distributed evenly across the reservoir area. In each of these cores, the first and second layers (0 to 4 cm deep, containing the fresher OC), the last sediment layer above the pre-flooding soil surface (containing the older OC) and one sample every ~8 cm in between (OC of intermediate age) were analyzed. This selection of layers for carbon and nitrogen analyses was motivated by the exponential decrease of OC mass loss rates during sediment degradation (Middelburg et al., 1993; Gälman et al., 2008). Linear interpolation was used to derive OC and TN concentrations of layers that were not measured.

Dried sediment samples were ground in a Planetary Ball Mill (Retsch PM 100) equipped with stainless steel cup and balls. Sediment was packed in pressed tin capsules and analyzed for TC and TN with a Costech 4010 elemental analyzer. The molar carbon to nitrogen (C:N) ratio in the surface layers was then calculated. The presence of carbonates was checked in the samples qualitatively by adding drops of acid and

checking visually for reaction. No evidence of solid carbonates was found, thus measurements of TC correspond to OC.

CH₄ concentration in pore water

The CH₄ concentration in pore water was measured according to Sobek et al., (2012) to determine if CH₄ is close to saturation concentration and, thus, prone to form gas bubbles. The saturation concentration, calculated here from temperature and pressure along the sediment profiles, represents the maximum concentration that dissolves in pore water, above which bubbles are formed. The presence of gas bubbles is indicative for an elevated probability of CH₄ ebullition, but not necessarily relates quantitatively to ebullition flux, since ebullition flux to the atmosphere is also dependent on water depth, sediment grain size, and pressure fluctuations (McGinnis et al., 2006; Maeck et al., 2014; Liu et al., 2016). The top 20 cm (February 2016) or 40 cm (September 2017) of the sediment cores were sampled every 2 cm. Deeper sediment was sampled every 4 cm until the bottom or pre-flooding material. Using a core liner with side ports, 2 ml of sediment were collected using a syringe with a cut-off tip, added to a 25 mL glass vial with 10 ml of distilled water, and closed with a 10 mm thick butyl rubber stopper. The slurry (2 mL sediment + 10 mL distilled water) was equilibrated with 13 mL headspace of ambient air (void volume of the glass vial) immediately after sampling by vigorously shaking the glass vial, and then the headspace was transferred to another syringe. The headspace was stored in the syringe, closed with a gas-tight valve, and then analyzed for CH₄ concentration within the same day using an Ultraportable Greenhouse Gas Analyzer (UGGA, Los Gatos Research) with a custom-made sample injection port. Then, the resulting peaks were integrated using R software (RStudio Version 1.1.383). The CH₄ concentration in the pore water was calculated from the headspace CH₄ concentration, based on the Henry's law constants. The

saturation concentration of CH₄ in each sediment layer was calculated based on air pressure, water depth, sediment temperature, and sample depth within the sediment core. The sediment layers with CH₄ concentrations above 100% saturation were considered as prone to ebullition. This is a conservative assumption because it is likely that a part of the CH₄ in the sediment was lost to the atmosphere due to pressure drop during core retrieval, as well as during sample processing.

Data analysis

The average sediment accumulation rate (SAR; cm yr⁻¹) was calculated for each of the 114 cores by dividing the thickness of the post-flooding sediment (cm) by the years since the reservoir construction (39 years in 2016 or 40 years in 2017), according to the equation:

$$\text{Sediment accumulation rate} = \frac{\text{sediment thickness}}{\text{reservoir age}}$$

This approach returns the average sediment accumulation rate over the lifetime of the reservoir (Renwick et al., 2005; Kunz et al., 2011; Mendonça et al., 2014; Quadra et al., 2019), and therefore incorporates any short-term variability in sediment deposition, for example, caused by an episodic change in sediment load or internal sediment movement. The large amount of core samples distributed evenly across the reservoir body also covers the spatial variability in sediment deposition, for example due to sediment focusing (sediment movement with preferential deposition in deeper areas).

OC burial rates (g C m⁻² yr⁻¹) were calculated for the sub-set of 19 sites where OC content was analyzed. OC mass (g C) in each sediment slice was calculated as OC content (g C g⁻¹) multiplied by dry sediment mass (g). Total OC mass (g C) in the cores

was the sum of OC mass in all post-flooding sediment layers. Then, the average OC burial rate ($\text{g C m}^{-2} \text{ yr}^{-1}$) for each of these 19 sites was calculated dividing the total OC mass in post-flooding sediment (g C) by the core surface area ($2.8 \times 10^{-3} \text{ m}^2$) and the reservoir age (yr) at the sampling dates, according to the equation:

$$\text{Organic carbon burial rate} = \frac{\text{OC in reservoir sediment}}{\text{core area} \times \text{reservoir age}}$$

The empirical relationship between SAR and OC burial rate (see Results; $y = 159x - 4.4$; $R^2 = 0.87$; Fig. S3) was used to estimate the OC burial rate ($\text{g C m}^{-2} \text{ yr}^{-1}$) for the remaining 95 coring sites where OC content was not analyzed.

To produce spatially-resolved maps of SAR and OC burial rate, the data from the 114 cores were interpolated to the reservoir area using the Inverse Distance Weighted algorithm (IDW, cell size of approximately $22 \text{ m} \times 22 \text{ m}$). From the spatially-resolved average OC burial rate, the reservoir age (40 years) and total flooded area (72 km^2), we calculated the total OC stock in the reservoir sediment. Using the same approach, we interpolated the pore water CH_4 concentration, and C:N ratio for the whole reservoir area. Spatial analyses were performed in ArcGIS 10.3.1 (ESRI).

To investigate any potential relationships between the land cover of sub-catchments and the spatial distribution of sediment characteristics and rates, land cover data were derived from maps of 1 km resolution (Global Land Cover Project, GLC2000), made available by the European Commission's science and knowledge service, including 23 land cover classes. The classes found in the CUN watershed were then grouped in three main classes: (1) forest (tree cover, natural vegetation, shrub, and herbaceous cover); (2) managed areas (cultivated and managed areas, cropland and bare

areas); (3) and water bodies. The extent of the CUN watershed and sub-catchments were identified using the WWF HydroBASINS tool (HydroSHEDS, 2019).

To verify the differences between CH₄ concentrations in the two seasons (rising and falling water), the non-parametric Wilcoxon Test was performed using the software JMP 14.1.0 (SAS).

Results

Water column profiles

The water column temperature profiles showed a average of 30 ± 1 °C, 29 ± 1 °C and 29 ± 2 °C (average \pm SD) in the surface, the middle and bottom layers, respectively. The dissolved oxygen average was 7 ± 1 mg L⁻¹, 6 ± 1 mg L⁻¹ and 5 ± 1 mg L⁻¹ in the surface, the middle and bottom layer, respectively. These water profiles suggest that the relatively shallow water column does not develop stable stratification over any extended periods of time, even if short-lived stratification events can occur (**Table S2**).

Sediment accumulation and organic carbon burial rates

SAR in the coring sites (n = 114) varied from 0 to 1.7 cm yr⁻¹ (0.6 ± 0.4 cm yr⁻¹, 95% confidence interval: 0.5-0.7 cm yr⁻¹; **Table S1**). In some areas of rocky or sandy bottom, especially near river inflows and along the main river bed, sediment could not be retrieved with our corer and SAR was considered as zero (total of 10 sites). OC burial rate in the coring sites (n = 114) varied from 0 to 269 g C m⁻² yr⁻¹ (91 ± 61 g C m⁻² yr⁻¹, 95% confidence interval: 80-102 g C m⁻² yr⁻¹; **Table S1**). The highest values of OC burial were observed near the dam, at the confluence of the major inflowing rivers, and in the inflow area of the main tributary, Curuá-Una River (**Fig. 1**). Our sampling was representative of the whole system, from the margins, where there is a greater

presence of dead tree trunks, to the river bed, where the sedimentation was lower (**Fig. 1**). Therefore, the simple average OC burial from the cores resulted in the same average OC burial rate derived from the spatial interpolation ($91 \text{ g C m}^{-1} \text{ yr}^{-1}$). The total burial rate for the CUN reservoir area was $6.5 \times 10^{10} \text{ g C yr}^{-1}$, corresponding to an accumulation of 0.3 Tg C in CUN sediments since its construction.

C:N ratio and land cover

The C:N ratio of the surface layers of sediment ($n = 19$), used as an indicator of organic matter source, varied from 10.3 to 17 (12.9 ± 2.1 , **Table S3**, **Fig. 2**). Higher C:N ratios were observed in the dam area and at the river inflows (**Fig. 2**).

Tropical rain forest was the dominant land cover in CUN, covering from 60.6 to 98.6% of the sub-catchment areas. Managed areas covered 1.4 to 40.9% of the sub-catchments areas, with the higher values occurring in the northwestern tributaries, which were also smaller compared to the southern ones (**Fig. 1**). Water surfaces covered 0.3% of the total CUN catchment area (**Table S4**).

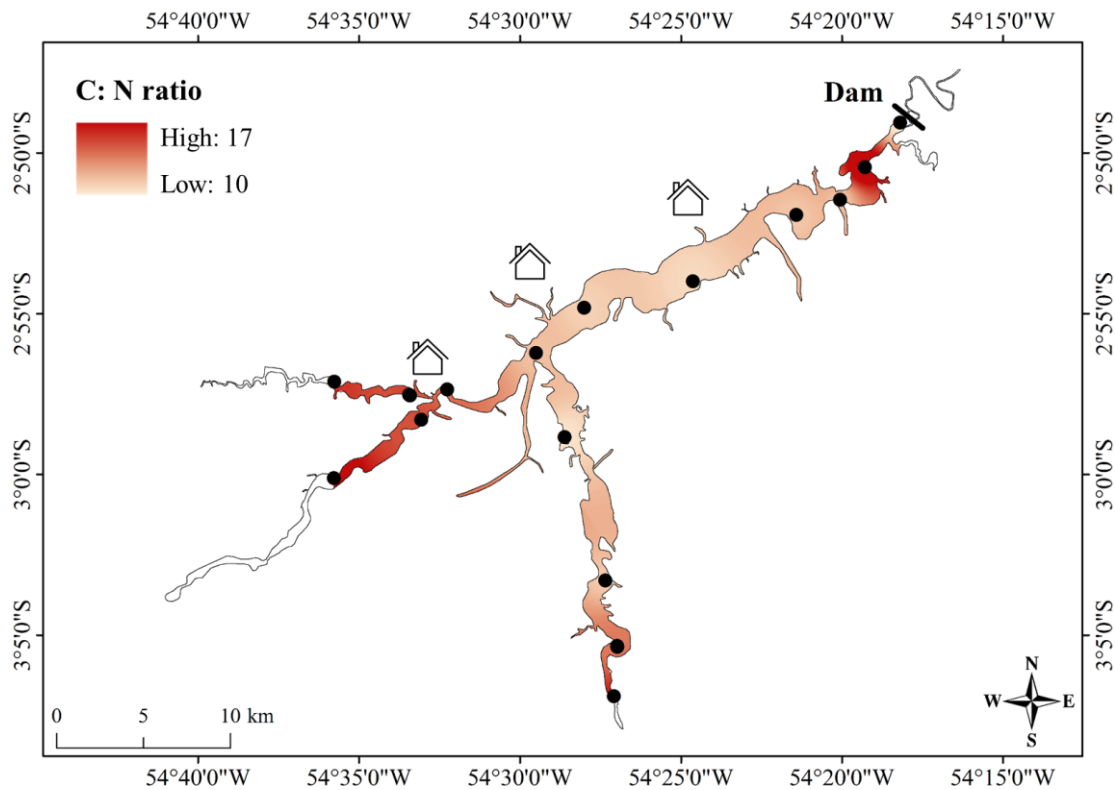


Figure 2. C:N ratio of surface sediment in Curuá-Una reservoir. The black dots represent the sampling sites. The houses represent the settlements at the reservoir.

Pore water CH₄ profiles and saturation

The overall average CH₄ concentration in pore water from CUN was $1\,729 \pm 1\,939 \mu\text{mol L}^{-1}$ of CH₄ with similar averages during rising ($1\,700 \pm 1\,637 \mu\text{mol L}^{-1}$ of CH₄, **Fig. S4**) and falling water ($1\,764 \pm 2\,243 \mu\text{mol L}^{-1}$ of CH₄, **Fig. S4**) periods. At eight sites, we could make paired observations of CH₄ concentration in sediment pore water at both rising and falling periods (**Fig. 3**). These data show that the seasonal difference of CH₄ concentration in pore water was low and not significant ($S = 33213$, $Z = -1.27863$, $\text{Prob} > |Z| = 0.20$). Of the 25 pore water CH₄ profiles, 20 contained at least one sample with pore water CH₄ above the 100% saturation concentration; of the total of 386 pore water samples, 90 samples (23%) were above the CH₄ saturation concentration. Pore water CH₄ saturation was higher in river inflow areas, especially in

314 sampling sites in the Curuá-Una main river. The confluence of the rivers and the dam
315 area were also characterized by high pore water CH₄ (**Fig. 4**). The widespread
316 appearance of gas bubbles in the sediment is in accordance with the sub-bottom profiler
317 data, which for a large part of the reservoir could not be used to identify sub-bottom
318 structures, because of a very strong acoustic reflector in surficial sediment, presumably
319 gas bubbles.

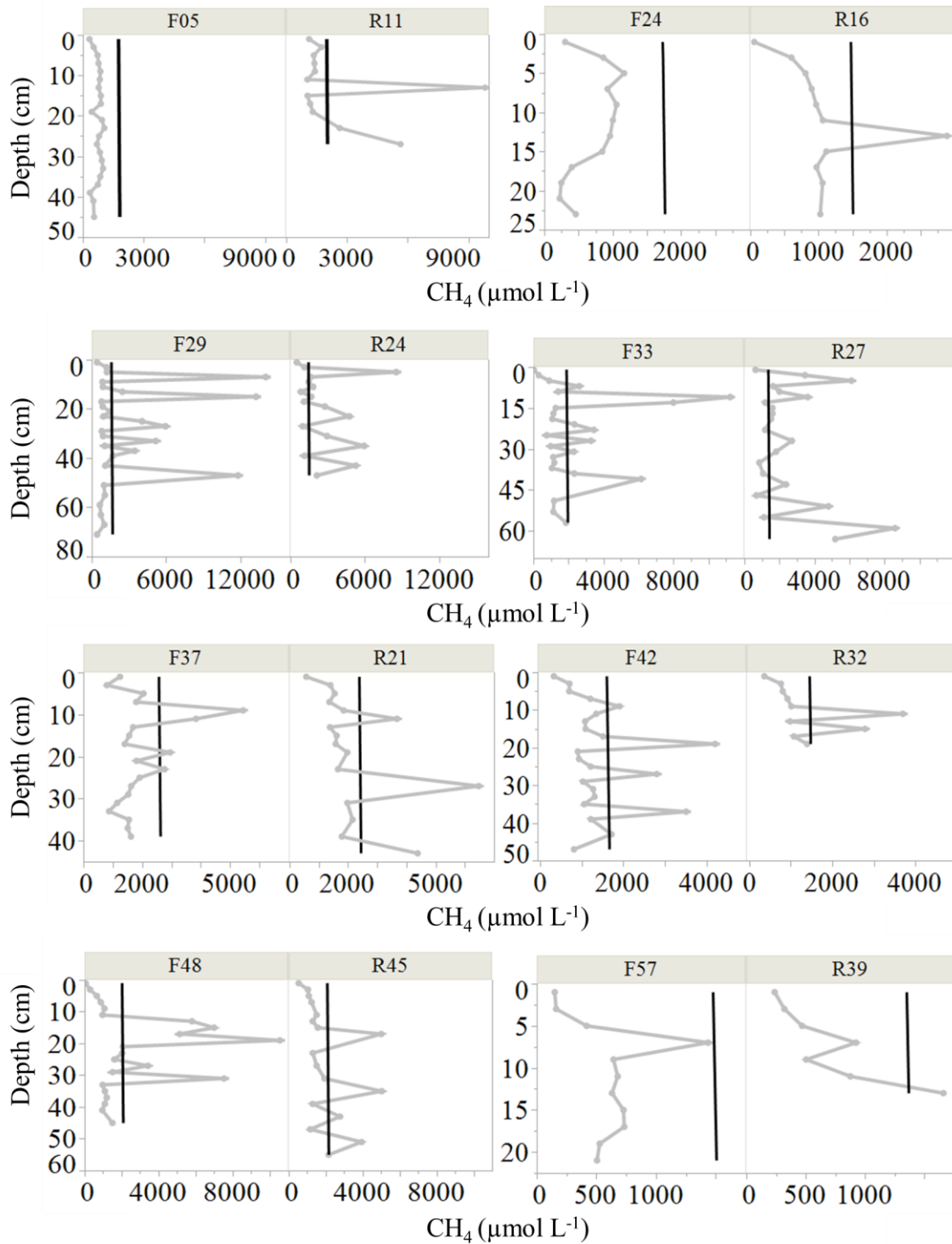


Figure 3. Paired observations of pore water CH_4 profiles during rising (R) and falling (F) water periods at eight different sampling sites across the reservoir. Black lines represent the CH_4 saturation concentration ($\mu\text{mol L}^{-1}$) and grey lines represent the

measured CH_4 concentration ($\mu\text{mol L}^{-1}$) over sediment depth. The numbers following the letters F and R correspond to the site codes in **Table S1**.

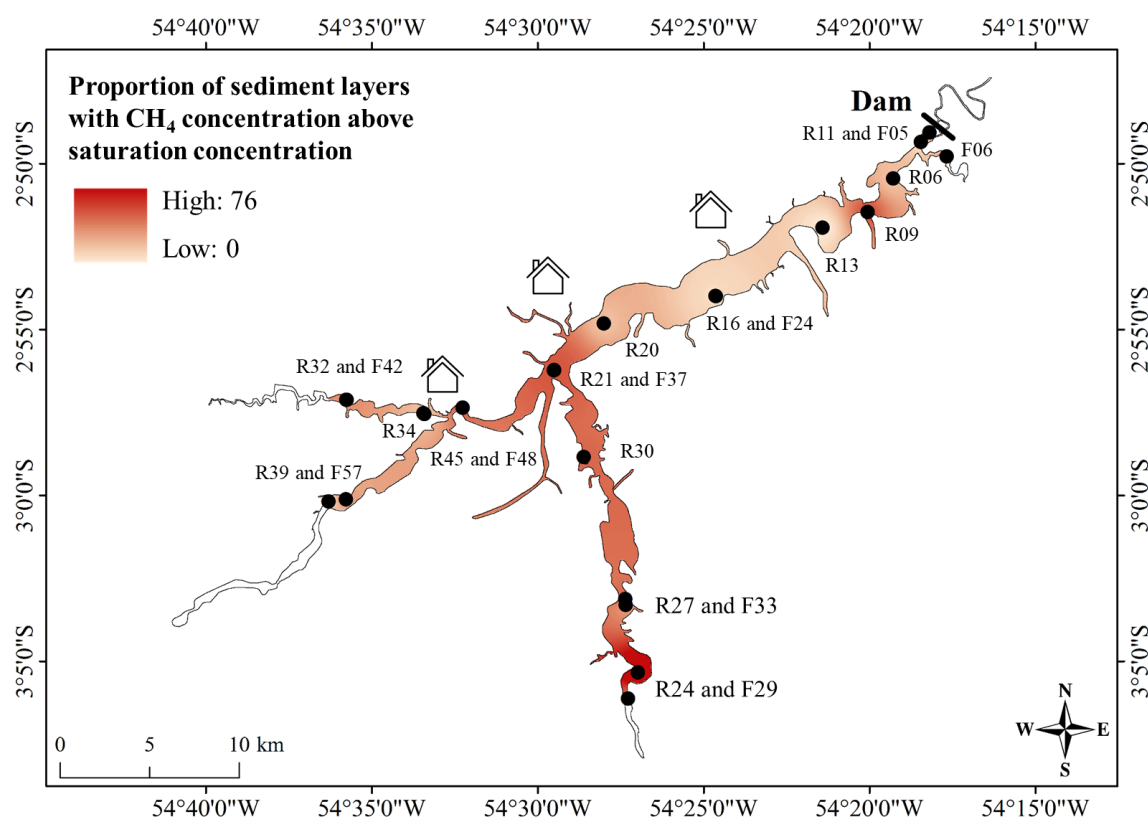


Figure 4. Percentage of sediment layers with CH_4 concentration above saturation. The black dots represent the sampling sites to produce the interpolation. The houses represent the settlements at the reservoir.

Discussion

Despite the intense OC mineralization in the tropics, this study found that OC burial in the sediment of the Amazonian Curuá-Una reservoir was high when compared to sub-tropical and other tropical reservoirs, probably due to the high carbon inputs from the forest. However, autochthonous material was also an important component of CUN sediment. CH_4 concentrations in the sediment pore-water were frequently

supersaturated, indicating that the sediment of CUN also has the potential to emit CH₄ to the atmosphere via ebullition.

SAR and OC burial in an Amazonian reservoir

When a river enters a reservoir, the water flow tends to decrease, favoring the deposition of suspended particles (Fisher, 1983; Scully et al., 2003). Typically, reservoir sedimentation rates are higher in the inflow areas and lower near the shores (Morris and Fan, 1998; Sedláček et al., 2016). CUN showed high SAR near the inflow areas, especially in the main tributary, but in contrast to other reservoirs (e.g. Mendonça et al., 2014), we did not observe any decrease in SAR towards the margins (i.e. the shore). In CUN, sediment accumulation across the entire reservoir area is favored by the shallow topography of the area, and by the presence of dead tree trunks along the reservoir including the margins, which reduce water flow and wave-driven resuspension. Accordingly, our data show that SAR was randomly distributed in relation to the water column depth (**Fig. S5**). Some reservoirs show higher sedimentation rates near the dam, which can be called ‘muddy lake area’ (Morris and Fan, 1998; Sedláček et al., 2016), and occurs in reservoirs where the fine sediment is transported all the way to the dam (Morris and Fan, 1998; Jenzer Althaus et al., 2009; Sedláček et al., 2016; Schleiss et al., 2016). CUN may be one of those cases (**Fig. 1**), possibly because water retention time is low in the main river channel which is narrow and well separated from the dead tree area, permitting transport of fine-grained sediment until the deeper dam area, where sediments tend to accumulate (Lehman, 1975; Blais and Kalff, 1995). Sediment accumulation was also high at the confluence of the three main tributaries (**Fig. 1**), probably due to sediment deposition as water flow slows down when the rivers enter the main body of the reservoir.

Although average SAR in CUN (0.6 cm yr^{-1}) was only slightly higher than that of non-Amazonian reservoirs in Brazil (e.g. Mendonça et al., 2014: 0.5 cm yr^{-1} ; Franklin et al., 2016: 0.4 cm yr^{-1}), OC burial rates were much higher in CUN than in other hydroelectric reservoirs in the tropics and sub-tropics. For example, OC burial was four times lower in Lake Kariba ($23 \text{ g C m}^{-2} \text{ yr}^{-1}$, Zimbabwe, Kunz et al., 2011) and about two times lower in Mascarenhas de Moraes ($42 \text{ g C m}^{-2} \text{ yr}^{-1}$, Brazil, Mendonça et al., 2014) and other Brazilian reservoirs ($40 \pm 28 \text{ g C m}^{-2} \text{ yr}^{-1}$, Brazil, Sikar et al., 2009) when compared to CUN. Even though natural lakes tend to bury OC at lower rates than artificial reservoirs (Mendonça et al., 2017), some Amazonian floodplain lakes showed higher OC burial rates than the CUN reservoir ($266 \pm 57 \text{ g C m}^{-2} \text{ yr}^{-1}$; Sanders et al., 2017). This is probably due to their smaller sizes which may result in a higher SAR since there is little area for sediment deposition, but high sediment load from the river during periods of high discharge. While a comparison with the latest global estimate of OC burial in reservoirs – median of $291 \text{ g C m}^{-2} \text{ yr}^{-1}$ (Mendonça et al., 2017) may lead to the conclusion that OC burial in CUN is low, it must be accounted that this global estimate (Mendonça et al., 2017) includes many small agricultural reservoirs (farm ponds), which are generally highly eutrophic systems that receive high sediment inputs from agriculture, resulting in extremely high OC burial rates (Downing et al., 2008). Hence, if compared to other hydroelectric reservoirs at low latitudes, our conclusion remains that OC burial in CUN is high. Importantly, comparisons of average SAR and OC burial rate between studies may be complicated by different sampling schemes, as sedimentation can vary in space and time (Radbourn et al., 2017; Stratton et al., 2019); for example, while in some studies, sites along the margins with zero sedimentation were sampled (e.g. Mendonça et al., 2014; our study), in other studies it was not (Moreira-Turcq et al., 2004; Knoll et al., 2014).

The high OC burial in CUN when compared to other low-latitude hydroelectric reservoirs is probably due to the high OC inputs from the productive Amazonian rain forest (Zhang et al., 2017), which compensates the intense sediment mineralization rates caused by high temperature. Using the linear regression model from a compilation of mineralization in freshwater sediments from the literature (Cardoso et al., 2014),

$$OC\ mineralization = (1.52 + 0.05) \times Temperature$$

and the average temperature of the bottom water in CUN (29°C), sediment OC mineralization is estimated at a average of 325 g C m⁻² yr⁻¹. This estimation assumes the same sample size as OC burial (n = 114), and consequently that the random error of each individual prediction (Cardoso et al., 2014) largely averages out and becomes negligible (<1 g C m⁻² yr⁻¹) for the average of predicted OC mineralization. This estimate of the average sediment OC mineralization rate is in the upper end of the range of values found for Brazilian reservoirs (Cardoso et al., 2014), but may even be conservative given that the CUN reservoir is located in a highly productive biome with high organic matter supply. The total OC deposition rate onto the sediment (OC mineralization + OC burial) of CUN is thus 418 g C m⁻² yr⁻¹, returning a estimated average OC burial efficiency of 22 % (OC burial efficiency = OC burial / OC deposition rate; Sobek et al., 2009). As expected, due to the positive effect of temperature on mineralization, the estimated average OC burial efficiency in the CUN reservoir is low in comparison to other reservoirs (at least 41% in the tropical lake Kariba (Kunz et al., 2011); average of 67% in the sub-tropical Mascarenhas de Moraes reservoir (Mendonça et al., 2016); average of 87% in the temperate lake Wohlen reservoir (Sobek et al., 2012)). A low OC burial efficiency allows high OC burial only if OC deposition onto

the sediment is high enough, and we suggest that the high productivity of the surrounding Amazonian rainforest constitutes a strong OC supply to CUN sediments.

The C:N ratio indicates that the sediment OC in CUN consists of a mixture of land-derived and internally-produced OC. The surface sediment C:N ratio varied from 10.3 to 17.0 (**Table S3**), and the C:N ratios of phytoplankton are typically 6-9, of aquatic macrophytes >10, of land plants >40 (Meyers and Ishiwatari, 1993; Grasset et al., 2019) and of Amazonian topsoils 10 to 14 (Batjes and Dijkshoorn, 1999). Although we refrained from making quantitative analysis based on C:N ratios, higher C:N values at the river inflow areas (**Fig. 2**) may indicate input from the highly productive watershed and thus the high load of land-derived OC to the sediment. Tropical rain forest is the dominant land cover in the CUN catchment (91%, **Fig. 1**), which may suggest that the high OC burial rates in CUN are related to a high OC input from the watershed. However, there was no strong relation between OC burial rate and C:N ratio (**Fig. S7A**), even though the C:N ratio has been shown to affect the OC burial efficiency (Sobek et al., 2009). Possibly, the strong effect of SAR on OC burial masked the potential effect of the C:N ratio. In addition, the middle section of the reservoir was characterized by relatively low C:N ratio, indicating a significant share of aquatic OC in the sediment (**Fig. 2**). Likely, the higher water transparency downstream from the river inflow areas due to particle settling stimulate aquatic primary production. Possibly, also sewage input from riverside communities (represented as houses in **Fig. 2**) contributes with N to the reservoir and thus further stimulates aquatic production, since a comparatively low C:N ratio was found near these settlements. Also, even at low C:N ratios, OC burial rates were high (**Fig. S6A**). Hence, it is evident that internally-produced OC makes up an important contribution to the OC buried in the sediments of CUN. The source of buried OC has an important implication in terms of accounting for

the sediment carbon as a new sink or not (Prairie et al., 2017), since the burial of aquatic OC can be ascribed to aquatic primary production in the reservoir, which would not have taken place in the absence of the dam, and thus represents a new carbon sink. However, our data do not allow us to make a quantitative estimate of the share of the CUN sediment carbon stock that is of aquatic origin, and thus may be accountable as a new carbon sink resulting from river damming (Prairie et al., 2017).

The spatial pattern of OC burial suggests that the catchment size affects sediment load and sedimentation, since the largest sub-catchment (6966 km²), entering CUN from the south, corresponds with high OC burial rates in the southern river inflow area (**Fig. 1**). The northwestern tributaries, which drain only 2111 and 300 km², are not associated with high OC burial in the northeastern tributary (**Fig. 1**), possibly because they are smaller, even though they have a higher share of managed land (34 and 41%, respectively) than the southern sub-catchment (4%). Apparently, even though land management increase erosion (Syvitski and Kettner, 2011), we cannot detect any such effect on sediment OC burial. Also concerning the C:N ratio, an effect of land cover is not evident, since the inflow area of the forest-dominated sub-catchment in the southwest (2855 km²; 99% forest) had a similar C:N ratio as the tributary of the northwestern sub-catchments, with their higher share of managed land. Possibly, the effect of land cover is masked by other factors affecting sediment OC and C:N, such as internal productivity and local particle settling patterns.

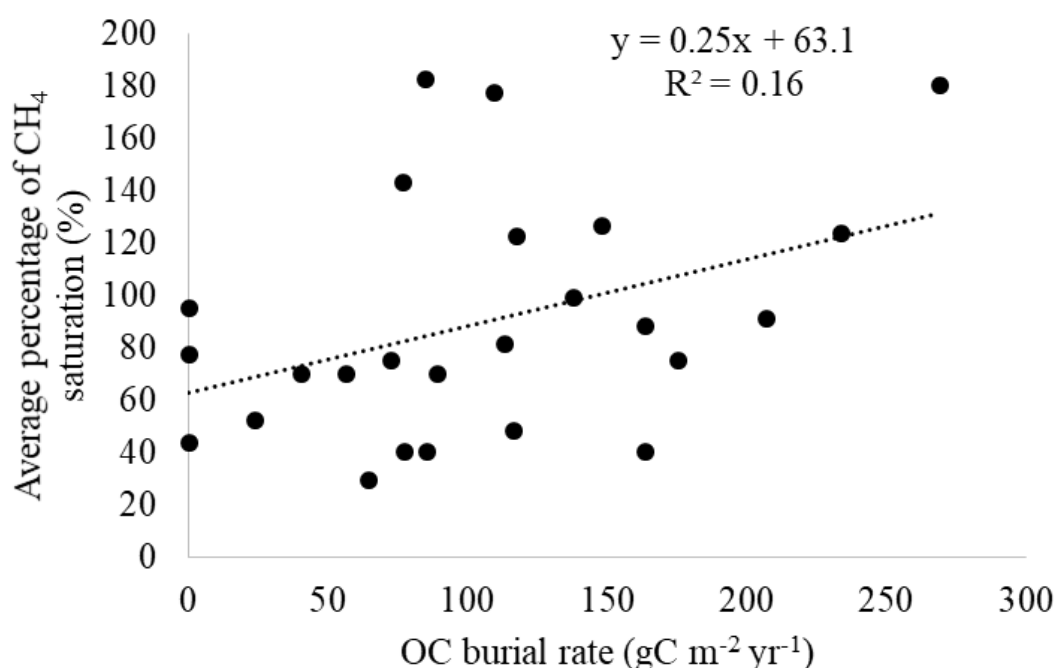
Despite being high compared to other hydroelectric reservoirs, OC burial in CUN represents only 15% of the total carbon emission to the atmosphere reported for the CUN reservoir (509 g C m⁻² yr⁻¹, Duchemin et al., 2000). Similarly, a study conducted in a boreal Canadian reservoir found that OC burial corresponded to 10% of reservoir carbon emission (Teodoru et al., 2012), although burial in other reservoirs can

be close to (70%, Mendonça et al., 2014) or even much higher than the total carbon emission to the atmosphere (1600%, Sobek et al., 2012). The magnitudes of carbon burial in relation to the emission in reservoirs depends on many factors (Mendonça et al., 2012). Therefore, although freshwater carbon emission tends to be consistently higher than OC burial in Amazonian freshwater systems (Mendonça et al., 2012), we cannot speculate in how far the results of this study applies to other reservoirs in the Amazon region since many factors affect the carbon processing in inland waters.

High potential for CH₄ ebullition

The high amount of pore water CH₄ profiles with samples above the CH₄ saturation concentration indicates a high likelihood of gas bubble formation in most of the sampled sites, and thus the possibility of CH₄ ebullition (**Table S5**). Importantly, however, the link between bubble presence in the sediment and CH₄ ebullition flux is entirely qualitative, and can not be used to estimate the magnitude of CH₄ ebullition. Sites with higher OC burial rate, i.e. river inflow areas, especially the Curuá-Una river, the confluence of the three main rivers and the dam area, also showed a tendency towards higher extent of CH₄ saturation (**Fig. 4**). However, while the relationship between average CH₄ saturation and OC burial at the different sites was positive, it was also weak, but clearly shows the overall high level of CH₄ saturation in CUN sediments (**Fig. 5**). Hence, the CH₄ production in CUN sediments may rather be influenced by the OC supply rate to anaerobic sediment layers than by the reactivity of the sediment OC, since there was no association between the C:N ratio and the extent of CH₄ saturation (**Fig. S7B**). Links between high sedimentation rate and sediment CH₄ pore water concentration as well as CH₄ ebullition have been reported previously (Sobek et al., 2012; Maeck et al., 2013), and in addition, fresh land plant-derived organic matter such as leaves transported by the rivers may fuel substantial CH₄ production at anoxic

conditions (Grasset et al., 2018). This highlights that sediment accumulation bottoms close to river inflow areas can be prone to exhibit high CH₄ ebullition (DelSontro et al., 2011), not least because the shallow water column in inflow areas (**Fig. S6**) facilitates CH₄ bubble transport to the atmosphere.



487

Figure 5. Regression model of average percentage of CH₄ saturation (%) in the sediment pore water and OC burial rate (g C m⁻² yr⁻¹). Each circle represents one sampling site.

Compared to other reservoirs, CUN had a higher share of sites (20 of 25) with pore water CH₄ concentration over the saturation threshold. In the Mascarenhas de Morais reservoir (Brazil), 6 of 16 sites with pore water CH₄ concentration over the saturation threshold were found (Mendonça et al., 2016). In Lake Wohlen (Switzerland), 4 of 8 sites with pore water CH₄ concentration over the threshold were found (Sobek et al., 2012). However, these differences should be interpreted with caution. Using the 100% saturation concentration as a threshold may underestimate the

potential for ebullition, since changes in the pressure may result in bubbles release during sediment sampling, especially in layers above 100% saturation. Therefore, our results of the degree of pore water CH₄ saturation, as well as the results from the literature cited above, are conservative.

We did not find statistical difference between CH₄ pore water concentration during rising and falling periods (**Fig. 3**), although other studies suggest a strong influence of water level or pressure changes on CH₄ ebullition (Mattson and Likens, 1990; Eugster et al., 2011; Maeck et al., 2014). Interestingly, 2 of the 8 sites with generally low CH₄ pore water concentration were low at both sampling occasions, indicating that there may be an important spatial component in sediment CH₄ production and saturation (**Fig. 3**, sites F24 x R16 and F57 x R39), which however was not related to the C:N ratio or OC burial rate at these sites.

Conclusions

The comparatively high OC burial rate of the Amazonian CUN reservoir probably results from high OC deposition onto the sediment, since the warm water (28-30°C) implies a high sediment OC mineralization rate. The forest seems to be a major OC source to the reservoir although the relatively low C:N ratio in some parts of the reservoir suggests an also significant aquatic contribution to sediment OC burial. In some parts of the reservoir, particularly in the river inflow areas, sediments are probably a CH₄ source by ebullition. Therefore, large inputs from a highly productive forest probably boost the OC burial rate, as well as CH₄ production, with a still unknown net effect on the regional carbon budget. Given the planned expansion of hydropower dams in the Amazon region, and the high OC burial rate in CUN shown here, future studies should quantify how OC burial and CH₄ emission may be affected by new Amazonian

hydroelectric reservoirs. Moreover, it will be critical to quantify the effect of the new Amazonian reservoirs on the ocean's carbon budget, since the CUN dam alone retains yearly 7,500 tons of OC and a part of it would likely reach the ocean in the absence of the dam.

Data availability. All the data used in this study can be found in the manuscript and in the Supplement.

Author contributions. GRQ, JRP, AI, RM, RV carried out the sampling campaigns. GRQ processed the data. AI analyzed the samples. GRQ and JRP prepared the figures. RM, SS, FR designed the study. All authors contributed to interpreting data and writing the manuscript.

Competing interests. The authors declare that they have no conflict of interest.

Acknowledgments. The research leading to these results has received funding from the European Research Council under the European Union's Seventh Framework Programme (FP7/2007–2013)/ERC grant agreement n° 336642. S.S. received additional support by the program *Pesquisador Visitante Especial, Ciência sem Fronteiras*, n° 401384/2014-4. This study was also financed in part by the *Coordenação de Aperfeiçoamento de Pessoal de Nível Superior* (CAPES) - Finance Code 001. F.R. has been supported by the *Conselho Nacional de Desenvolvimento Científico e Tecnológico* (CNPq; grant no. 401384/2014-4). We are thankful for the support from ELETRONORTE during the field campaigns.

References

Aben, R. C., Barros, N., Van Donk, E., Frenken, T., Hilt, S., Kazanjian, G., Lamers, L. P., Peeters, E. T., Roelofs, J. G., and de Senerpont Domis, L. N.: Cross continental

- 545 increase in methane ebullition under climate change, *Nature communications*, 8, 1682,
546 2017.
- 547 Almeida, R. M., Barros, N., Cole, J. J., Tranvik, L., and Roland, F.: Emissions from
548 Amazonian dams, *Nature Climate Change*, 3, 1005, 2013.
- 549 Almeida, R. M., Shi, Q., Gomes-Selman, J. M., Wu, X., Xue, Y., Angarita, H., Barros,
550 N., Forsberg, B. R., García-Villacorta, R., Hamilton, S. K., Melack, J. M., Montoya, M.,
551 Perez, G., Sethi, S. A., Gomes, C. P., Flecker, A. S. Reducing greenhouse gas emissions
552 of Amazon hydropower with strategic dam planning. *Nature communications*, 10, 1-9.
553 2019.
- 554 Barros, N., Cole, J. J., Tranvik, L. J., Prairie, Y. T., Bastviken, D., Huszar, V. L., Del
555 Giorgio, P., and Roland, F.: Carbon emission from hydroelectric reservoirs linked to
556 reservoir age and latitude, *Nature Geoscience*, 4, 593, 2011.
- 557 Batjes, N. H., and Dijkshoorn, J. A.: Carbon and nitrogen stocks in the soils of the
558 Amazon Region, *Geoderma*, 89, 273-286, 1999.
- 559 Blais, J. M., and Kalff, J.: The influence of lake morphometry on sediment focusing,
560 *Limnology and Oceanography*, 40, 582-588, 1995.
- 561 Cardoso, S. J., Enrich-Prast, A., Pace, M. L., and Roland, F.: Do models of organic
562 carbon mineralization extrapolate to warmer tropical sediments?, *Limnology and*
563 *Oceanography*, 59, 48-54, 2014.
- 564 Cole, J. J., Prairie, Y. T., Caraco, N. F., McDowell, W. H., Tranvik, L. J., Striegl, R. G.,
565 Duarte, C. M., Kortelainen, P., Downing, J. A., and Middelburg, J. J.: Plumbing the

- 566 global carbon cycle: integrating inland waters into the terrestrial carbon budget,
567 *Ecosystems*, 10, 172-185, 2007.
- 568 da Silva Soito, J. L., and Freitas, M. A. V.: Amazon and the expansion of hydropower
569 in Brazil: Vulnerability, impacts and possibilities for adaptation to global climate
570 change, *Renewable and Sustainable Energy Reviews*, 15, 3165-3177, 2011.
- 571 Deemer, B. R., Harrison, J. A., Li, S., Beaulieu, J. J., DelSontro, T., Barros, N.,
572 Bezerra-Neto, J. F., Powers, S. M., Dos Santos, M. A., and Vonk, J. A.: Greenhouse gas
573 emissions from reservoir water surfaces: a new global synthesis, *BioScience*, 66, 949-
574 964, 2016.
- 575 DelSontro, T., Boutet, L., St-Pierre, A., del Giorgio, P. A., and Prairie, Y. T.: Methane
576 ebullition and diffusion from northern ponds and lakes regulated by the interaction
577 between temperature and system productivity, *Limnology and Oceanography*, 61, S62-
578 S77, 2016.
- 579 DelSontro, T., Kunz, M. J., Kempter, T., Wüest, A., Wehrli, B., and Senn, D. B.: Spatial
580 heterogeneity of methane ebullition in a large tropical reservoir, *Environmental science*
581 *& technology*, 45, 9866-9873, 2011.
- 582 Downing, J. A., Cole, J. J., Duarte, C., Middelburg, J. J., Melack, J. M., Prairie, Y. T.,
583 Kortelainen, P., Striegl, R. G., McDowell, W. H., and Tranvik, L. J.: Global abundance
584 and size distribution of streams and rivers, *Inland waters*, 2, 229-236, 2012.
- 585 Downing, J. A., Cole, J. J., Middelburg, J. J., Striegl, R. G., Duarte, C. M., Kortelainen,
586 P., Prairie, Y. T., and Laube, K. A.: Sediment organic carbon burial in agriculturally
587 eutrophic impoundments over the last century, *Global Biogeochemical Cycles*, 22,
588 2008.

- 589 Duchemin, É., Lucotte, M., Canuel, R., Queiroz, A. G., Almeida, D. C., Pereira, H. C.,
590 and Dezincourt, J.: Comparison of greenhouse gas emissions from an old tropical
591 reservoir with those from other reservoirs worldwide. *Internationale Vereinigung für*
592 *theoretische und angewandte Limnologie: Verhandlungen*, 27, 1391-1395, 2000.
- 593 Eugster, W., DelSontro, T., and Sobek, S.: Eddy covariance flux measurements confirm
594 extreme CH₄ emissions from a Swiss hydropower reservoir and resolve their short-term
595 variability. *Biogeosciences*, 8, 2815-2831, 2011.
- 596 Fearnside, P. M., and Pueyo, S.: Greenhouse-gas emissions from tropical dams, *Nature*
597 *Climate Change*, 2, 382, 2012.
- 598 Fearnside, P. M.: Do hydroelectric dams mitigate global warming? The case of Brazil's
599 Curuá-Una Dam, *Mitigation and Adaptation Strategies for Global Change*, 10, 675-691,
600 2005.
- 601 Fisher, R. V.: Flow transformations in sediment gravity flows, *Geology*, 11, 273-274,
602 1983.
- 603 Franklin, R. L., Fávaro, D. I. T., and Damatto, S. R.: Trace metal and rare earth
604 elements in a sediment profile from the Rio Grande Reservoir, Sao Paulo, Brazil:
605 determination of anthropogenic contamination, dating, and sedimentation rates, *Journal*
606 *of Radioanalytical and Nuclear Chemistry*, 307, 99-110, 2016.
- 607 Gälman, V., Rydberg, J., de-Luna, S. S., Bindler, R., and Renberg, I.: Carbon and
608 nitrogen loss rates during aging of lake sediment: changes over 27 years studied in
609 varved lake sediment, *Limnology and Oceanography*, 53, 1076-1082, 2008.

- 610 Grasset, C., Abril, G., Mendonça, R., Roland, F., and Sobek, S.: The transformation of
 611 macrophyte-derived organic matter to methane relates to plant water and nutrient
 612 contents, *Limnology and Oceanography*, 2019.
- 613 Grasset, C., Mendonça, R., Villamor Saucedo, G., Bastviken, D., Roland, F., and Sobek,
 614 S.: Large but variable methane production in anoxic freshwater sediment upon addition
 615 of allochthonous and autochthonous organic matter, *Limnology and oceanography*, 63,
 616 1488-1501, 2018.
- 617 HydroBASINS: <https://www.hydrosheds.org/page/hydrobasins>, 2019.
- 618 IPCC: Stocker, T. F., Qin, D., Plattner, G. K., Tignor, M., Allen, S. K., Boschung, J.,
 619 Nauels, A., Xia, Y., Bex, V., Midgley, P. M. *Climate change 2013: The physical science*
 620 *basis*, 2013.
- 621 Jenzer Althaus, J., De Cesare, G., Boillat, J.-L., and Schleiss, A.: Turbidity currents at
 622 the origin of reservoir sedimentation, case studies, *Proceedings (on CD) of the 23rd*
 623 *Congress of the Int. Commission on Large Dams CIGB-ICOLD*, 58-60, 2009.
- 624 Knoll, L. B., Vanni, M. J., Renwick, W. H., and Kollie, S.: Burial rates and
 625 stoichiometry of sedimentary carbon, nitrogen and phosphorus in M idwestern US
 626 reservoirs, *Freshwater biology*, 59, 2342-2353, 2014.
- 627 Kortelainen, P., Rantakari, M., Pajunen, H., Huttunen, J. T., Mattsson, T., Juutinen, S.,
 628 Larmola, T., Alm, J., Silvola, J., and Martikainen, P. J.: Carbon evasion/accumulation
 629 ratio in boreal lakes is linked to nitrogen, *Global Biogeochemical Cycles*, 27, 363-374,
 630 2013.

- 631 Kunz, M. J., Anselmetti, F. S., Wüest, A., Wehrli, B., Vollenweider, A., Thüring, S.,
632 and Senn, D. B.: Sediment accumulation and carbon, nitrogen, and phosphorus
633 deposition in the large tropical reservoir Lake Kariba (Zambia/Zimbabwe), *Journal of*
634 *Geophysical Research: Biogeosciences*, 116, 2011.
- 635 Lehman, J. T.: Reconstructing the Rate of Accumulation of Lake Sediment: The Effect
636 of Sediment Focusing 1, *Quaternary Research*, 5, 541-550, 1975.
- 637 Liu, L., Wilkinson, J., Koca, K., Buchmann, C., and Lorke, A.: The role of sediment
638 structure in gas bubble storage and release, *Journal of Geophysical Research:*
639 *Biogeosciences*, 121, 1992-2005, 2016.
- 640 Maeck, A., DelSontro, T., McGinnis, D. F., Fischer, H., Flury, S., Schmidt, M., Fietzek,
641 P., and Lorke, A.: Sediment trapping by dams creates methane emission hot spots,
642 *Environmental science & technology*, 47, 8130-8137, 2013.
- 643 Maeck, A., Hofmann, H., and Lorke, A.: Pumping methane out of aquatic sediments:
644 Ebullition forcing mechanisms in an impounded river, *Biogeosciences*, 11, 2925-2938,
645 2014.
- 646 Marotta, H., Pinho, L., Gudas, C., Bastviken, D., Tranvik, L. J., and Enrich-Prast, A.:
647 Greenhouse gas production in low-latitude lake sediments responds strongly to
648 warming, *Nature Climate Change*, 4, 467, 2014.
- 649 Mattson, M. D., and Likens, G. E.: Air pressure and methane fluxes. *Nature*, 347, 718,
650 1990.

- 651 McGinnis, D. F., Greinert, J., Artemov, Y., Beaubien, S., and Wüest, A.: Fate of rising
 652 methane bubbles in stratified waters: How much methane reaches the atmosphere?,
 653 *Journal of Geophysical Research: Oceans*, 111, 2006.
- 654 Mendonça, R., Kosten, S., Sobek, S., Barros, N., Cole, J. J., Tranvik, L., and Roland, F.:
 655 Hydroelectric carbon sequestration, *Nature Geoscience*, 5, 838, 2012.
- 656 Mendonça, R., Kosten, S., Sobek, S., Cardoso, S. J., Figueiredo-Barros, M. P., Estrada,
 657 C. H. D., and Roland, F.: Organic carbon burial efficiency in a large tropical
 658 hydroelectric reservoir, *Biogeosciences*, 13, 3331-3342, 2016.
- 659 Mendonça, R., Kosten, S., Sobek, S., Cole, J. J., Bastos, A. C., Albuquerque, A. L.,
 660 Cardoso, S. J., and Roland, F.: Carbon sequestration in a large hydroelectric reservoir:
 661 an integrative seismic approach, *Ecosystems*, 17, 430-441, 2014.
- 662 Mendonça, R., Müller, R. A., Clow, D., Verpoorter, C., Raymond, P., Tranvik, L. J.,
 663 and Sobek, S.: Organic carbon burial in global lakes and reservoirs, *Nature*
 664 *communications*, 8, 1694, 2017.
- 665 Meyers, P. A., and Ishiwatari, R.: Lacustrine organic geochemistry—an overview of
 666 indicators of organic matter sources and diagenesis in lake sediments, *Organic*
 667 *geochemistry*, 20, 867-900, 1993.
- 668 Middelburg, J. J., Vlug, T., Jaco, F., and Van der Nat, W. A.: Organic matter
 669 mineralization in marine systems, *Global and Planetary Change*, 8, 47-58, 1993.
- 670 Moreira-Turcq, P., Jouanneau, J., Turcq, B., Seyler, P., Weber, O., and Guyot, J.-L.:
 671 Carbon sedimentation at Lago Grande de Curuai, a floodplain lake in the low Amazon

- 672 region: insights into sedimentation rates, *Palaeogeography, Palaeoclimatology,*
 673 *Palaeoecology*, 214, 27-40, 2004.
- 674 Morris, G. L., and Fan, J.: Reservoir sedimentation handbook: design and management
 675 of dams, reservoirs, and watersheds for sustainable use, McGraw Hill Professional,
 676 1998.
- 677 Mulholland, P. J., and Elwood, J. W.: The role of lake and reservoir sediments as sinks
 678 in the perturbed global carbon cycle, *Tellus*, 34, 490-499, 1982.
- 679 Paranaíba, J. R., Barros, N., Mendonça, R., Linkhorst, A., Isidorova, A., Roland, F.,
 680 Almeida, R. M., and Sobek, S.: Spatially resolved measurements of CO₂ and CH₄
 681 concentration and gas-exchange velocity highly influence carbon-emission estimates of
 682 reservoirs, *Environmental science & technology*, 52, 607-615, 2018.
- 683 Prairie, Y. T., Alm, J., Beaulieu, J., Barros, N., Battin, T., Cole, J., Del Giorgio, P.,
 684 DelSontro, T., Guérin, F., and Harby, A.: Greenhouse gas emissions from freshwater
 685 reservoirs: what does the atmosphere see?, *Ecosystems*, 1-14, 2017.
- 686 Quadra, G. R., Lino, A., Sobek, A., Malm, O., Barros, N., Guida, Y., Thomaz, J.,
 687 Mendonça, R., Cardoso, S., Estrada, C., Rust, F., and Roland, F.: Environmental Risk of
 688 Metal Contamination in Sediments of Tropical Reservoirs. *Bulletin of Environmental*
 689 *Contamination and Toxicology*, 1-10, 2019.
- 690 Radbourne, A. D., Ryves, D. B., Anderson, N. J., and Scott, D. R.: The historical
 691 dependency of organic carbon burial efficiency, *Limnology and Oceanography*, 62,
 692 1480-1497, 2017.

- Raymond, P. A., Hartmann, J., Lauerwald, R., Sobek, S., McDonald, C., Hoover, M.,
Butman, D., Striegl, R., Mayorga, E., and Humborg, C.: Global carbon dioxide
emissions from inland waters, *Nature*, 503, 355, 2013.
- Renwick, W. H., Smith, S. V., Bartley, J. D., and Buddemeier, R. W.: The role of
impoundments in the sediment budget of the conterminous United States.
Geomorphology, 71, 99-111, 2005.
- Sanders, L. M., Taffs, K. H., Stokes, D. J., Sanders, C. J., Smoak, J. M., Enrich-Prast,
A., Macklin, P. A., Santos, I. R., and Marotta, H.: Carbon accumulation in Amazonian
floodplain lakes: A significant component of Amazon budgets?, *Limnology and
Oceanography Letters*, 2, 29-35, 2017.
- Schleiss, A. J., Franca, M. J., Juez, C., and De Cesare, G.: Reservoir sedimentation,
Journal of Hydraulic Research, 54, 595-614, 2016.
- Scully, M., Friedrichs, C. T., and Wright, L.: Numerical modeling of gravity-driven
sediment transport and deposition on an energetic continental shelf: Eel River, northern
California, *Journal of Geophysical Research: Oceans*, 108, 2003.
- Sedláček, J., Bábek, O., and Kielar, O.: Sediment accumulation rates and high-
resolution stratigraphy of recent fluvial suspension deposits in various fluvial settings,
Morava River catchment area, Czech Republic, *Geomorphology*, 254, 73-87, 2016.
- Segers, R.: Methane production and methane consumption: a review of processes
underlying wetland methane fluxes. *Biogeochemistry*, 41, 23-51, 1998.
- Sikar, E., Matvienko, B., Santos, M., Rosa, L., Silva, M., Santos, E., Rocha, C., and
Bentes Jr, A.: Tropical reservoirs are bigger carbon sinks than soils, *Internationale*

- 715 Vereinigung für theoretische und angewandte Limnologie: Verhandlungen, 30, 838-
716 840, 2009.
- 717 Sobek, S., DelSontro, T., Wongfun, N., and Wehrli, B.: Extreme organic carbon burial
718 fuels intense methane bubbling in a temperate reservoir, *Geophysical Research Letters*,
719 39, 2012.
- 720 Sobek, S., Durisch-Kaiser, E., Zurbrügg, R., Wongfun, N., Wessels, M., Pasche, N., and
721 Wehrli, B.: Organic carbon burial efficiency in lake sediments controlled by oxygen
722 exposure time and sediment source, *Limnology and Oceanography*, 54, 2243-2254,
723 2009.
- 724 Sobek, S., Zurbrügg, R., and Ostrovsky, I.: The burial efficiency of organic carbon in
725 the sediments of Lake Kinneret, *Aquatic sciences*, 73, 355-364, 2011.
- 726 Stratton, L. E., Haggerty, R., and Grant, G. E.: The Importance of Coarse Organic
727 Matter and Depositional Environment to Carbon Burial Behind Dams in Mountainous
728 Environments. *Journal of Geophysical Research: Earth Surface*, 124, 2118-2140, 2019.
- 729 Syvitski, J. P., and Kettner, A.: Sediment flux and the Anthropocene. *Philosophical*
730 *Transactions of the Royal Society A: Mathematical, Physical and Engineering Sciences*,
731 369, 957-975, 2011.
- 732 Team, R. C. R: A language and environment for statistical computing. Vienna, Austria:
733 R Foundation for Statistical Computing; 2017, ISBN3-900051-07-0 [https://www. R-](https://www.R-project.Org)
734 [project. Org](https://www.R-project.Org).
- 735 Teodoru, C. R., Bastien, J., Bonneville, M. C., del Giorgio, P. A., Demarty, M.,
736 Garneau, M., Hélie, J. F., Pelletier, L., Prairie, Y. T., and Roulet, N. T.: The net carbon

- 737 footprint of a newly created boreal hydroelectric reservoir, *Global Biogeochemical*
 738 *Cycles*, 26, 2012.
- 739 Tranvik, L. J., Downing, J. A., Cotner, J. B., Loiselle, S. A., Striegl, R. G., Ballatore, T.
 740 J., Dillon, P., Finlay, K., Fortino, K., and Knoll, L. B.: Lakes and reservoirs as
 741 regulators of carbon cycling and climate, *Limnology and Oceanography*, 54, 2298-
 742 2314, 2009.
- 743 Verpoorter, C., Kutser, T., Seekell, D. A., and Tranvik, L. J.: A global inventory of
 744 lakes based on high-resolution satellite imagery, *Geophysical Research Letters*, 41,
 745 6396-6402, 2014.
- 746 Vörösmarty, C. J., Meybeck, M., Fekete, B., Sharma, K., Green, P., and Syvitski, J. P.:
 747 Anthropogenic sediment retention: major global impact from registered river
 748 impoundments, *Global and planetary change*, 39, 169-190, 2003.
- 749 Wik, M., Thornton, B. F., Bastviken, D., MacIntyre, S., Varner, R. K., and Crill, P. M.:
 750 Energy input is primary controller of methane bubbling in subarctic lakes, *Geophysical*
 751 *Research Letters*, 41, 555-560, 2014.
- 752 Winemiller, K. O., McIntyre, P. B., Castello, L., Fluet-Chouinard, E., Giarrizzo, T.,
 753 Nam, S., Baird, I., Darwall, W., Lujan, N., and Harrison, I.: Balancing hydropower and
 754 biodiversity in the Amazon, Congo, and Mekong, *Science*, 351, 128-129, 2016.
- 755 Yvon-Durocher, G., Allen, A. P., Bastviken, D., Conrad, R., Gudas, C., St-Pierre, A.,
 756 Thanh-Duc, N., and Del Giorgio, P. A.: Methane fluxes show consistent temperature
 757 dependence across microbial to ecosystem scales, *Nature*, 507, 488, 2014.

- 758 Zarfl, C., Lumsdon, A. E., Berlekamp, J., Tydecks, L., and Tockner, K.: A global boom
759 in hydropower dam construction, *Aquatic Sciences*, 77, 161-170, 2015.
- 760 Zhang, Y., Xiao, X., Wu, X., Zhou, S., Zhang, G., Qin, Y., and Dong, J.: A global
761 moderate resolution dataset of gross primary production of vegetation for 2000–2016,
762 *Scientific data*, 4, 2017.